Electron Transport

Deutsche Ausgabe: DOI: 10.1002/ange.201500972
Internationale Ausgabe: DOI: 10.1002/anie.201500972

Synthesis, Structure, and Air-stable N-type Field-Effect Transistor Behaviors of Functionalized Octaazanonacene-8,19-dione**

*Chengyuan Wang, Jing Zhang, Guankui Long, Naoki Aratani, Hiroko Yamada, Yang Zhao, and Qichun Zhang**

Dedicated to Professor Fred Wudl on the occasion of his 75th birthday

Abstract: *Increasing the length of N-heteroacenes or their analogues is highly desirable because such materials could have great potential applications in organic electronics. In this report, the large π-conjugated N-heteroquinone 6,10,17,21-tetra-((triisopropylsilyl)ethynyl)-5,7,9,11,16,18,20,22-octaazanonacene-8,19-dione (OANQ) has been synthesized and characterized. The as-prepared OANQ shows high stability under ambient conditions and has a particularly low LUMO level, which leads to it being a promising candidate for air-stable n-type field-effect transistors (FETs). In fact, FET devices based on OANQ single crystals have been fabricated and an electron mobility of up to 0.2 $cm^2 V^{-1} s^{-1}$ under ambient conditions is reported. More importantly, no obvious degradation was observed even after one month. Theoretical calculations based on the single crystal are consistent with the measured mobility.*

Organic field-effect transistors (OFETs) have attracted a lot of attention because of their applications in flexible and large-area organic electronics such as radio frequency identification (RFID) tags,[1] optical displays,[2] electronic papers,[3] various sensors,[4] and so on. Although OFETs have several advantages, including device flexibility and low fabrication cost, the poor operational stability (sensitivity to oxygen, moisture, or light) of certain OFETs has imposed a limitation on their practical applications. Such problems are particularly true for electron-transport (n-type) OFETs.[5] To address this issue, various organic semiconducting materials have been designed and synthesized, including fullerene-based acceptors,[6] oligoacenes modified with electron-withdrawing substitutes,[7] imide- or amide-functionalized small molecules and polymers,[8] 7,7,8,8-tetracyanoquinodimethane (TCNQ) and its analogues,[9] etc. However, up to now, few of them have fulfilled the requirement of being the ultimate FET material (air-stable, easy to process, owning high electron mobility, and good stability). Thus, it is highly desirable to search for novel organic materials to fill the gap.

Recently, large N-heteroacenes have proven to be promising ambipolar or n-type semiconducting materials.[10] A series of novel N-heteroacenes have been explored and high electron mobility under vacuum or inert atmosphere was achieved. However, it is still challenging to find a suitable N-heteroacene with good air-stable performance.[11] To our knowledge, lowering the LUMO level of the materials is the most effective way to prevent electron trapping by either O_2 or H_2O, and realize high electron transport in air. To achieve these features, introducing more-electron-withdrawing sp^2 N atoms into the backbone of N-heteroacenes or building up large conjugated systems has been investigated.[11b,12] Unfortunately, larger azacenes have poor stability and can be degraded either by moisture or oxygen, as well as through Diels–Alder reactions.[13] Compared to the parent N-heteroacene, large linearly-fused N-heteroquinones with relatively moderate conjugation levels could be a solution to breaking the deadlock because 1) large π-conjugated backbones in N-heteroquinones could lead to more efficient electron transport because of strong π–π interactions; 2) the lower LUMO level could be achieved by introducing more sp^2 N atoms into the backbone of N-heteroquinones; and 3) good air stability could be realized because of their moderate conjugation. Given these factors, we were interested in preparing a large, stable N-heteroquinone, 6,10,17,21-tetra-((triisopropylsilyl)-ethynyl)-5,7,9,11,16,18,20,22-octaazanonacene-8,19-dione (OANQ), having eight sp^2 N atoms in the backbone. The as-prepared OANQ shows very good electron-transport ability

[*] C. Wang,[+] Dr. J. Zhang,[+] Dr. G. Long, Prof. Dr. Y. Zhao, Prof. Dr. Q. Zhang
School of Materials Science and Engineering
Nanyang Technological University Singapore
639798 Singapore (Singapore)
E-mail: qczhang@ntu.edu.sg
Prof. Dr. N. Aratani, Prof. Dr. H. Yamada
Graduate School of Materials Science
Nara Institute of Science and Technology
Ikoma, 630-0192 (Japan)
Prof. Dr. Q. Zhang
Division of Chemistry and Biological Chemistry
School of Physical and Mathematical Sciences
Nanyang Technological University
Singapore 637371 (Singapore)
[+] These authors contributed equally to this work.

[**] We thank Changli Chen and Prof. Zhigang Shuai (Tsinghua University) for their assistance in the transfer integral calculation, Si Yu Tan and Prof. Yanli Zhao (Nanyang Technological University) for their assistance in HR mass analysis. Q.Z. acknowledges the financial support AcRF Tier 1 (RG 16/12 and RG RG133/14) and Tier 2 (ARC 20/12 and ARC 2/13) from MOE, CREATE program (Nanomaterials for Energy and Water Management) from NRF, and New Initiative Fund from NTU, Singapore. Y.Z. acknowledges the support from the Singapore National Research Foundation under Project No. NRF-CRP5-2009-04.

Supporting information for this article is available on the WWW under http://dx.doi.org/10.1002/anie.201500972.

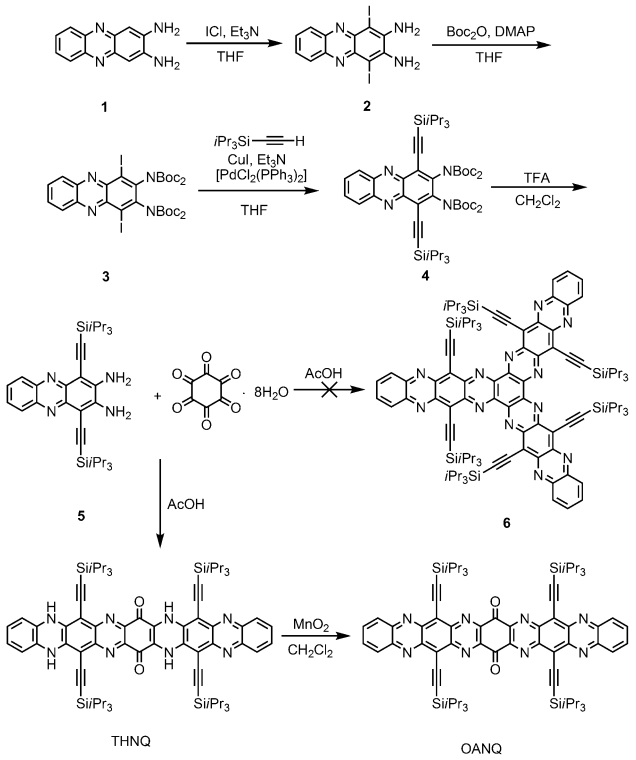

Scheme 1. Synthetic route to OANQ. Boc = tert-butoxycarbonyl, TFA = trifluoroacetic acid, THF = tetrahydrofuran.

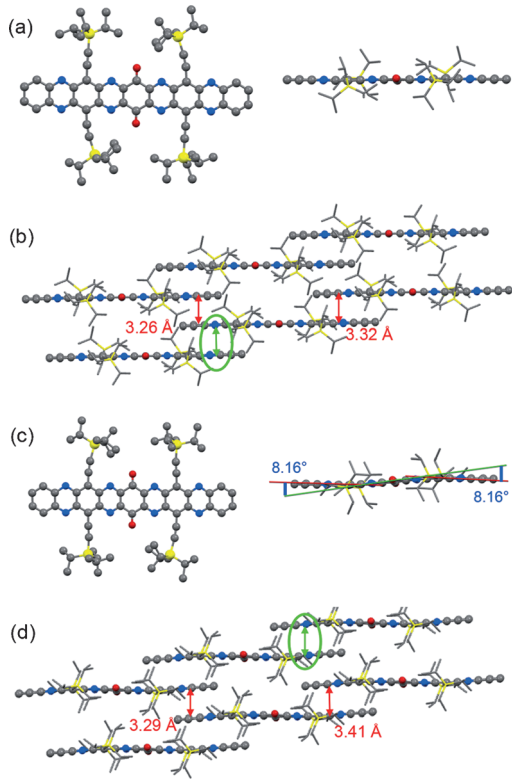

Figure 1. Single-crystal structures[20] of a) THNQ (left: top view; right: side view) and c) OANQ (left: top view, right: side view). Molecular stacking patterns of b) THNQ and d) OANQ.

with high operational stability when open to air. Such N-heteroquinone systems could provide novel insight into synthesizing large, stable conjugated systems for air-stable n-type transistors.

Scheme 1 shows the synthetic route to OANQ. The compound **5** was prepared according a literature procedure.[11b] The intermediate 6,10,17,21-tetra-[(triisopropylsilyl)ethynyl]-5,9,18,22-tetrahydro-5,7,9,11,16,18,20,22-octaazanonacene-9,10-dione (THNQ) was obtained as a dark-blue powder in 21.7% yield through a one-step condensation reaction between **5** and hexaketocyclohexane octahydrate (HKCO). In a previous study, when HKCO reacted with *o*-phenylenediamine derivatives, hexaazatrinaphthylene derivatives were obtained as the main product.[14] However, herein we believe that the steric effect of (triisopropylsilyl)ethynyl (TIPS) substitutes allows **5** to attack HKCO from the *para*-position. The hypothesis was verified when THNQ was obtained as the main product and the compound **6** was not observed. The hydrogen atoms attached to the nitrogen atoms of the pyrazine rings are located at the 5-, 9-, 18-, and 22-positions, and are confirmed by ^{1}H NMR spectroscopy, thus indicating that this arrangement would make THNQ more stable. Further oxidation of THNQ with MnO_2 gave OANQ as a dark-green powder in 91.1% yield. Both THNQ and OANQ are characterized by high-resolution mass spectroscopy (HRMS), ^{1}H and ^{13}C NMR spectroscopy (see the Supporting Information), and single-crystal analysis.

Platelike single crystals of THNQ and OANQ were obtained through slowly diffusing acetonitrile into a toluene solution. The molecular structures and stacking patterns are shown in Figure 1. All hydrogen atoms and solvent molecules are omitted for clarification. No obvious difference could be observed from the top views of the THNQ and OANQ structures, however, in the side views, THNQ displays a perfect plane conformation while OANQ shows a slightly twisted configuration with one tetraazaacene unit bent up and the other one bent down relative to the quinone center at a dihedral angle at 8.16°. Such a twisted configuration of the OANQ backbone is probably important for the enhancement of the stability of the long linear molecular structure and stacking by releasing molecular strain generated from the π interactions and bulky substituents. The neighboring THNQ molecules adopt a face-to-face two-dimensional (2D) "bricklayer" arrangement with unsymmetrical overlapping areas, and the interplanar distances are 3.26 and 3.32 Å, thus suggesting the existence of strong π–π interactions. A similar molecular stacking mode is observed in OANQ, but with slightly longer π–π distances (3.29 Å and 3.41 Å), which might be due to the twisted configuration. Compared to the spatial arrangement of THNQ molecules, OANQ molecules have more areas overlapping with each other (see cycle region), thus leading to stronger π–π interactions. Since the 2D face-to-face stacking and strong π–π interactions are favored for large transfer integrals and 2D electron transport, good electron transporting properties of OANQ in the solid state can be expected.[15]

Figure 2a shows the normalized UV-vis absorption spectra of THNQ and OANQ in CH_2Cl_2. THNQ has three absorption bands at $\lambda = 494$, 551, and 599 nm. The strong and

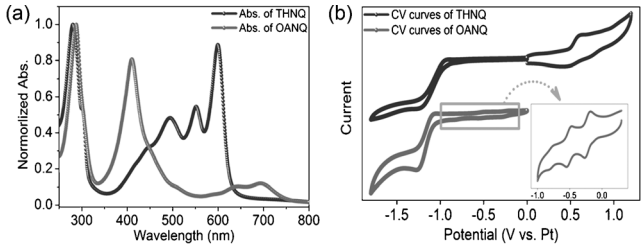

Figure 2. a) UV/Vis absorption spectra of TANQ and OANQ in CH_2Cl_2. b) Cyclic voltammetric (CV) curves of THNQ and OANQ in CH_2Cl_2/0.1 M nBu_4NPF_6. Scanning speed: 50 mV s^{-1}.

broad absorption from $\lambda = 400$ to 630 nm suggests the existence of intramolecular charge transfer. The onset of absorption (λ_{onset}) at $\lambda = 632$ nm determines the optical band gap as 1.96 eV. OANQ shows one strong absorption peak at $\lambda = 409$ nm, and two small peaks at $\lambda = 641$ and 694 nm. The optical band gap is determined to be 1.65 eV from the λ_{onset} value at 753 nm. Clearly, OANQ has a longer λ_{onset} value than TIPS-pentacene and its analogues, but shorter λ_{onset} value than typical hexacene and its N-substituted counterpart, thus suggesting that it has a relatively moderate conjugation.[10c,11b,16]

The electrochemical properties of THNQ and OANQ were investigated by cyclic voltammetry (CV). As shown in Figure 2b, THNQ has one irreversible oxidative peak with an onset potential (E_{onset}) at 0.24 V [all the potentials are illustrated versus $FeCp_2^+/FeCp_2$ (Fc^+/Fc) unless otherwise specified] and one irreversible reductive peak ($E_{onset} = -1.19$ V). The HOMO level is determined from the E_{onset} value of the oxidative peak to be 5.04 eV and the LUMO is calculated to be −3.08 eV from the difference between the HOMO and optical band gap. OANQ displays no oxidative peak, but three small reversible reductive peaks with a half-wave potential ($E_{1/2}$) at −0.48 V, −0.77 V, and −1.05 V, and one irreversible reductive peak ($E_{onset} = -1.33$ V) were clearly observed. The LUMO level of OANQ is determined to be −4.32 eV from the $E_{1/2}$ value of the first reversible reductive peak. Accounting for the difference in the optical band gap and LUMO level, the HOMO level is determined to be −6.01 eV. Table 1 summarizes the

Table 1: The summarized energy levels for THNQ and OANQ.

Molecule	HOMO [eV][a]	LUMO [eV][a]	Gap [eV][a]	HOMO [eV][b]	LUMO [eV][b]	Gap [eV][b]	λ_{onset} [nm]
THNQ	−5.04	−3.08	1.96	−4.96	−3.08	1.87	632
OANQ	−6.01	−4.32	1.65	−5.68	−3.92	1.75	753

[a] Experimental results. [b] DFT calculated results (B3LYP/6-31G*).

experimental and calculated energy levels of THNQ and OANQ. The calculated HOMO and LUMO levels of THNQ are in good agreement with the experimental results, while those of OANQ are about 0.4 eV higher. The optical band gap deduced from calculations shows only a slight difference compared to the experimental results. The electron density distributions of THNQ and OANQ are illustrated in Figure S6 (see the Supporting Information). The HOMO levels of THNQ and OANQ are delocalized throughout the whole molecule. The LUMO of THNQ is mainly located at the quinone center, while that of OANQ is delocalized throughout the whole molecule. In addition, high electron density can be observed in the quinone center of OANQ, and implies that the quinone moiety possibly also plays an important role in lowering the LUMO level together with the sp^2 N atoms. The lower LUMO energy level and well-delocalized π electrons suggest that OANQ might have great potential for use in FETs as an air-stable n-type material.

Single-crystal FETs, which can better stand for the intrinsic property of molecules considering the smaller number of grain boundaries and defects in crystals than in films, were fabricated to investigate the electron-transport ability of THNQ and OANQ. The microcrystals suitable for device fabrication were prepared through a drop-casting method on a self-assembled octadecyltrichlorosilane (OTS) treated SiO_2/Si surface. Because THNQ has no detectable mobility under our research conditions, it will not be discussed. Micrometer-sized sheetlike crystals of OANQ were obtained with a width ranging from several to hundreds of micrometers and thicknesses at around several tens of nanometers (Figure 3a).

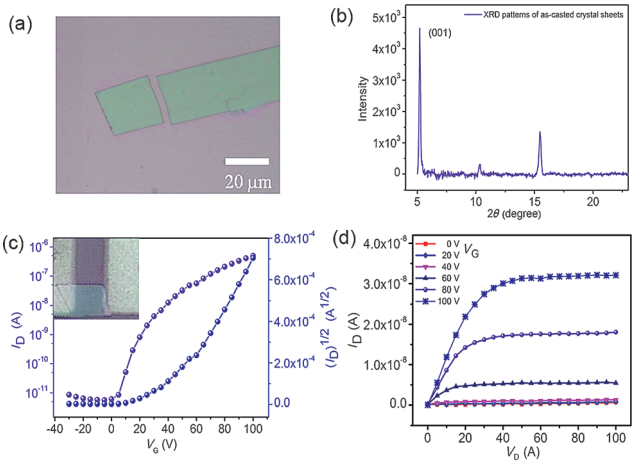

Figure 3. a) Image of the as-casted OANQ crystal sheet. b) XRD patterns of as-casted OANQ crystal sheets. c) Transfer and d) output curves of a typical device based on OANQ (for typical device setup see inset in (c)).

Powder X-ray diffraction (XRD) patterns of the as-casted crystal sheets are shown in Figure 3b. Strong Bragg reflections with intensities of up to 10^3–10^4 could be observed at 5.20°, 10.35°, and 15.50°, which were indexed as (001), (002), and (003), respectively. The sharp diffraction peak at 5.20° corresponded to the d-spacing of 1.68 nm, thus suggesting that OANQ nearly adopted an edge-on molecular orientation on the substrate, and crystallized into a 2D architecture with π–π and van der Waals interactions as driving forces. Transmission electron microscopy (TEM) and selected-area electron diffraction (SAED) were conducted to further investigate the packing orientation of OANQ. Figure S7 shows the SAED

patterns of a microcrystal grown on an amorphous carbon-coated TEM grid. The patterns of the crystal at different spots showed identical diffraction characteristics, thus indicating its high crystalline quality.

Bottom-contact FETs were fabricated with Ag as the source and drain electrodes to align its work function (−4.2 eV) with the LUMO level of OANQ (−4.32 eV). A copper grid with a patterned gap of 20 μm was used as a shadow mask. All the devices exhibited typical n-type behavior under ambient air, and the representative transfer and output characteristics are shown in Figure 3c and d. Based on the transfer curves, the highest electron-transport mobility (μ_e) is determined to be 0.2 $cm^2V^{-1}s^{-1}$ with an on/off ratio up to 10^5. Here μ was calculated in the saturation regime by using the equation: $I_D = \mu C_i(W/2L)(V_G - V_T)^2$, where I_D is the drain-source current, μ is the field-effect mobility, C_i is the gate dielectric capacitance, V_G is the gate voltage, V_T is the threshold voltage, and W and L are the channel width and length, respectively. It should be mentioned that all FETs based on OANQ exhibited excellent air stability and no obvious degradation was observed even after storage for one month under ambient conditions.

To understand the structure–property relationship of OANQ, theoretical calculations with the Marcus electron-transfer theory and an incoherent Brownian motion model were employed to deduce the hole and electron mobility[17] (see the Supporting Information) based on the single-crystal structure. The hole and electron reorganization energies are calculated to be 125.3 meV and 110.2 meV at the DFT/B3LYP/6-31G* level.[18] The room-temperature hole and electron-diffusion mobilities were obtained to be 0.19 $cm^2V^{-1}s^{-1}$ and 2.50 $cm^2V^{-1}s^{-1}$, respectively. The simulated electron mobility is inconsistent with the measured mobility of 0.2 $cm^2V^{-1}s^{-1}$, and π–π stacking directions (1, 2 and 3, 4 in Figure S8) showed the largest transfer integrals for electron transport of 33.73 and 15.32 meV, which is even close to the well-known perylene diimide (PDI) type n-type semiconductors with transfer integrals of about 50 meV.[19]

In summary, the large π-conjugated N-heteroquinone OANQ has been successfully synthesized and characterized. The as-prepared OANQ displays a particularly low LUMO level and good environmental stability. The existence of a slight twist on the backbone was believed to have an important contribution to stabilizing the molecular packing. The single-crystal FETs of OANQ showed electron-transport mobilities of up to 0.2 $cm^2V^{-1}s^{-1}$ under ambient conditions and maintained good performance stability. Our results suggest that the design and synthesis of large π-conjugated N-heteroquinones could be a promising way to develop new air-stable n-type materials for FET devices.

Keywords: conjugation · density functional calculations · electron transport · heterocycles · X-ray diffraction

How to cite: *Angew. Chem. Int. Ed.* **2015**, *54*, 6292–6296
Angew. Chem. **2015**, *127*, 6390–6394

[1] G. Gelinck, P. Heremans, K. Nomoto, T. D. Anthopoulos, *Adv. Mater.* **2010**, *22*, 3778–3798.

[2] a) G. H. Gelinck, H. E. Huitema, E. van Veenendaal, E. Cantatore, L. Schrijnemakers, J. B. van der Putten, T. C. Geuns, M. Beenhakkers, J. B. Giesbers, B. H. Huisman, E. J. Meijer, E. M. Benito, F. J. Touwslager, A. W. Marsman, B. J. van Rens, D. M. de Leeuw, *Nat. Mater.* **2004**, *3*, 106–110; b) H. E. A. Huitema, G. H. Gelinck, J. van der Putten, K. E. Kuijk, C. M. Hart, E. Cantatore, P. T. Herwig, A. van Breemen, D. M. de Leeuw, *Nature* **2001**, *414*, 599–599.

[3] a) B. Comiskey, J. D. Albert, H. Yoshizawa, J. Jacobson, *Nature* **1998**, *394*, 253–255; b) D. Tobjörk, R. Osterbacka, *Adv. Mater.* **2011**, *23*, 1935–1961.

[4] a) T. Someya, A. Dodabalapur, J. Huang, K. C. See, H. E. Katz, *Adv. Mater.* **2010**, *22*, 3799–3811; b) A. N. Sokolov, M. E. Roberts, Z. A. Bao, *Mater. Today* **2009**, *12*, 12–20; c) L. Torsi, M. Magliulo, K. Manoli, G. Palazzo, *Chem. Soc. Rev.* **2013**, *42*, 8612–8628.

[5] a) C. R. Newman, C. D. Frisbie, D. A. da Silva, J. L. Brédas, P. C. Ewbank, K. R. Mann, *Chem. Mater.* **2004**, *16*, 4436–4451; b) J. Zaumseil, H. Sirringhaus, *Chem. Rev.* **2007**, *107*, 1296–1323; c) J. E. Anthony, A. Facchetti, M. Heeney, S. R. Marder, X. Zhan, *Adv. Mater.* **2010**, *22*, 3876–3892.

[6] a) R. C. Haddon, A. S. Perel, R. C. Morris, T. T. M. Palstra, A. F. Hebard, R. M. Fleming, *Appl. Phys. Lett.* **1995**, *67*, 121–123; b) C. Waldauf, P. Schilinsky, M. Perisutti, J. Hauch, C. J. Brabec, *Adv. Mater.* **2003**, *15*, 2084–2088; c) R. C. Haddon, *J. Am. Chem. Soc.* **1996**, *118*, 3041–3042.

[7] a) M. L. Tang, Z. Bao, *Chem. Mater.* **2011**, *23*, 446–455; b) M. L. Tang, A. D. Reichardt, N. Miyaki, R. M. Stoltenberg, Z. Bao, *J. Am. Chem. Soc.* **2008**, *130*, 6064–6065; c) Y. Sakamoto, T. Suzuki, M. Kobayashi, Y. Gao, Y. Fukai, Y. Inoue, F. Sato, S. Tokito, *J. Am. Chem. Soc.* **2004**, *126*, 8138–8140.

[8] a) X. Guo, A. Facchetti, T. J. Marks, *Chem. Rev.* **2014**, *114*, 8943–9021; b) W. Jiang, Y. Li, Z. Wang, *Acc. Chem. Res.* **2014**, *47*, 3135–3147; c) X. Zhan, A. Facchetti, S. Barlow, T. J. Marks, M. A. Ratner, M. R. Wasielewski, S. R. Marder, *Adv. Mater.* **2011**, *23*, 268–284; d) Y. Zhao, Y. Guo, Y. Liu, *Adv. Mater.* **2013**, *25*, 5372–5391.

[9] a) A. R. Brown, D. M. Deleeuw, E. J. Lous, E. E. Havinga, *Synth. Met.* **1994**, *66*, 257–261; b) Q. Wu, R. Li, W. Hong, H. Li, X. Gao, D. Zhu, *Chem. Mater.* **2011**, *23*, 3138–3140; c) Y. Suzuki, E. Miyazaki, K. Takimiya, *J. Am. Chem. Soc.* **2010**, *132*, 10453–10466; d) F. Zhang, Y. Hu, T. Schuettfort, C.-a. Di, X. Gao, C. R. McNeill, L. Thomsen, S. C. B. Mannsfeld, W. Yuan, H. Sirringhaus, D. Zhu, *J. Am. Chem. Soc.* **2013**, *135*, 2338–2349; e) T. He, M. Stolte, F. Wuerthner, *Adv. Mater.* **2013**, *25*, 6951–6955; f) T. Lei, J.-H. Dou, X.-Y. Cao, J.-Y. Wang, J. Pei, *J. Am. Chem. Soc.* **2013**, *135*, 12168–12171; g) J. Xiao, Y. Azumal, Y. Liu, G. Li, F. Wei, K. J. Tan, C. Kloc, H. Zhang, Y. Majima, Q. Zhang, *Aust. J. Chem.* **2012**, *65*, 1674–1678.

[10] a) Y.-Y. Liu, C.-L. Song, W.-J. Zeng, K.-G. Zhou, Z.-F. Shi, C.-B. Ma, F. Yang, H.-L. Zhang, X. Gong, *J. Am. Chem. Soc.* **2010**, *132*, 16349–16351; b) C.-L. Song, C.-B. Ma, F. Yang, W.-J. Zeng, H.-L. Zhang, X. Gong, *Org. Lett.* **2011**, *13*, 2880–2883; c) Z. Liang, Q. Tang, J. Xu, Q. Miao, *Adv. Mater.* **2011**, *23*, 1535–1539.

[11] a) U. H. F. Bunz, J. U. Engelhart, B. D. Lindner, M. Schaffroth, *Angew. Chem. Int. Ed.* **2013**, *52*, 3810–3821; *Angew. Chem.* **2013**, *125*, 3898–3910; b) B. D. Lindner, J. U. Engelhart, O. Tverskoy, A. L. Appleton, F. Rominger, A. Peters, H.-J. Himmel, U. H. F. Bunz, *Angew. Chem. Int. Ed.* **2011**, *50*, 8588–8591; *Angew. Chem.* **2011**, *123*, 8747–8750; c) U. H. F. Bunz, *Chem. Eur. J.* **2009**, *15*, 6780–6789; d) Z. Liang, Q. Tang, R. Mao, D. Liu, J. Xu, Q. Miao, *Adv. Mater.* **2011**, *23*, 5514–5518; e) G. Li, J. Miao, J. Cao, J. Zhu, B. Liu, Q. Zhang, *Chem. Commun.* **2014**, *50*, 7656–7658; f) J. Li, P. Li, J. Wu, J. Gao, W. Xiong, G. Zhang, Y. Zhao, Q. Zhang, *J. Org. Chem.* **2014**, *79*, 4438–4445; g) G. Li, H. M. Duong, Z. Zhang, J. Xiao, L. Liu, Y. Zhao, H. Zhang, F. Huo, S. Li, J. Ma, F. Wudl, Q. Zhang, *Chem. Commun.* **2012**, *48*, 5974–

5976; h) Q. Zhang, J. Xiao, Z. Y. Yin, H. M. Duong, F. Qiao, F. Boey, X. Hu, H. Zhang, F. Wudl, *Chem. Asian J.* **2011**, *6*, 856 – 862.

[12] a) J. U. Engelhart, O. Tverskoy, U. H. Bunz, *J. Am. Chem. Soc.* **2014**, *136*, 15166 – 15169; b) P.-Y. Gu, F. Zhou, J. Gao, G. Li, C. Wang, Q.-F. Xu, Q. Zhang, J.-M. Lu, *J. Am. Chem. Soc.* **2013**, *135*, 14086 – 14089; c) Y. Fogel, M. Kastler, Z. Wang, D. Andrienko, G. J. Bodwell, K. Muellen, *J. Am. Chem. Soc.* **2007**, *129*, 11743 – 11749; d) G. Li, Y. Wu, J. Gao, C. Wang, J. Li, H. Zhang, Y. Zhao, Y. Zhao, Q. Zhang, *J. Am. Chem. Soc.* **2012**, *134*, 20298 – 20230; e) Y. Wu, Z. Yin, J. Xiao, Y. Liu, F. Wei, K. J. Tan, C. Kloc, L. Huang, Q. Yan, F. Hu, H. Zhang, Q. Zhang, *ACS Appl. Mater. Interfaces* **2012**, *4*, 1883 – 1886; f) A. Mateo-Alonso, N. Kulisic, G. Valenti, M. Marcaccio, F. Paolucci, M. Prato, *Chem. Asian J.* **2010**, *5*, 482 – 485; g) B. Gao, M. Wang, Y. Cheng, L. Wang, X. Jing, F. Wang, *J. Am. Chem. Soc.* **2008**, *130*, 8297 – 8306; h) G. Li, Y. Wu, J. Gao, J. Li, Y. Zhao, Q. Zhang, *Chem. Asian J.* **2013**, *8*, 1574 – 1578; i) G. Li, J. Gao, F. Hu, Q. Zhang, *Tetrahedron Lett.* **2014**, *55*, 282 – 285; j) J. Li, Y. Zhao, J. Lu, G. Li, J. Zhang, Y. Zhao, X. Sun, Q. Zhang, *J. Org. Chem.* **2015**, *80*, 109 – 113.

[13] a) Z. He, R. Mao, D. Liu, Q. Miao, *Org. Lett.* **2012**, *14*, 4190 – 4193; b) J. U. Engelhart, B. D. Lindner, O. Tverskoy, F. Rominger, U. H. F. Bunz, *Org. Lett.* **2012**, *14*, 1008 – 1011.

[14] S. Barlow, Q. Zhang, B. R. Kaafarani, C. Risko, F. Amy, C. K. Chan, B. Domercq, Z. A. Starikova, M. Y. Antipin, T. V. Timofeeva, B. Kippelen, J.-L. Brédas, A. Kahn, S. R. Marder, *Chem. Eur. J.* **2007**, *13*, 3537 – 3547.

[15] H. Dong, X. Fu, J. Liu, Z. Wang, W. Hu, *Adv. Mater.* **2013**, *25*, 6158 – 6183.

[16] J. E. Anthony, J. S. Brooks, D. L. Eaton, S. R. Parkin, *J. Am. Chem. Soc.* **2001**, *123*, 9482 – 9483.

[17] a) W. Q. Deng, W. A. Goddard, *J. Phys. Chem. B* **2004**, *108*, 8614 – 8621; b) J. L. Brédas, D. Beljonne, V. Coropceanu, J. Cornil, *Chem. Rev.* **2004**, *104*, 4971 – 5003; c) R. A. Marcus, *Rev. Mod. Phys.* **1993**, *65*, 599 – 610.

[18] Y. Song, C. a. Di, X. Yang, S. Li, W. Xu, Y. Liu, L. Yang, Z. Shuai, D. Zhang, D. Zhu, *J. Am. Chem. Soc.* **2006**, *128*, 15940 – 15941.

[19] H. Geng, Q. Peng, L. Wang, H. Li, Y. Liao, Z. Ma, Z. Shuai, *Adv. Mater.* **2012**, *24*, 3568 – 3572.

[20] CCDC 1046845 (THNQ) and CCDC 1046846 (OANQ) contain the supplementary crystallographic data for this paper. These data can be obtained free of charge from The Cambridge Crystallographic Data Centre via www.ccdc.cam.ac.uk/data_request/cif.

Received: February 2, 2015
Revised: March 8, 2015
Published online: March 31, 2015

